

## $\text{Ge}^{73}(n, \gamma)\text{Ge}^{74}$ Gamma-Ray Spectrum and Energy Levels of $\text{Ge}^{74}\dagger$

A. P. MAGRUDER\* AND R. K. SMITHER

*Argonne National Laboratory, Argonne, Illinois 60439*

(Received 12 July 1968; revised manuscript received 20 March 1969)

The  $\gamma$ -ray spectra resulting from thermal-neutron capture in targets of natural germanium and enriched  $\text{Ge}^{73}$  were measured with a  $\text{Ge}(\text{Li})$  germanium detector. The energies and intensities of 85  $\gamma$  rays in the energy range 0.20–3.00 MeV and 47  $\gamma$  rays in the range 6.1–9.6 MeV were identified with the reaction  $\text{Ge}^{73}(n, \gamma)\text{Ge}^{74}$ . The  $\gamma$ -ray spectrum was used to suggest four new levels, and place limits on the spins and parities of three other levels. Errors in the  $\gamma$ -ray energy values were reduced to less than 3 keV in all cases, and to less than 1 keV for many. Based on this experiment and other information, the energy levels identified below 3 MeV were 0.0 ( $0^+$ ), 596.3 ( $2^+$ ), 1204.9 ( $2^+$ ), 1466.2 ( $4^+$ ), [1486 ( $0^+$ )], [1697.7], 1699.9 ( $3^+$ ,  $4^+$ ), 2168.3 ( $3^+$ ,  $4^+$ ), 2200.2 ( $2^+$ ), 2539.3 ( $3^-$ ), 2574.1, 2672.4, [2695.8], 2699.1, 2833.2, 2929.2, 2939.7, and 2978.1 keV, where the levels in brackets were not fed directly from the capture state. The level energies were determined to within 1 keV. The energy of the capture state in the compound nucleus ( $\text{Ge}^{73}+n$ ) was found to be  $10\,203.1 \pm 0.9$  keV.

### I. INTRODUCTION

THE energy-level structure of  $\text{Ge}^{74}$  was investigated by means of the  $\text{Ge}^{73}(n, \gamma)\text{Ge}^{74}$  reaction, making use of the  $\text{Ge}(\text{Li})$  detector and in-pile sample facility at the Argonne Research Reactor CP-5. Other approaches have already provided many details of the level scheme. Ythier *et al.*<sup>1</sup> studied the  $\text{Ga}^{74} \rightarrow \text{Ge}^{74}$   $\beta$ -decay reaction and defined the energies and probable spins of five excited states in  $\text{Ge}^{74}$  below 3 MeV. The experiments of Eichler *et al.*<sup>2</sup> with the  $\text{Ga}^{74} \rightarrow \text{Ga}^{74}$  and the  $\text{As}^{74} \rightarrow \text{Ge}^{74}$   $\beta$ -decay reaction confirmed these findings and added two levels below 3 MeV, as well as six more above 3 MeV. Darcey's measurements<sup>3</sup> of the angular distribution of protons in the  $\text{Ge}^{74}(p, p')\text{Ge}^{74}$  and the  $\text{Ge}^{72}(t, p)\text{Ge}^{74}$  reactions established a  $0^+$  level at 1486 keV and a  $3^-$  level at 2537 keV, and provided evidence for three other new levels. The nature of the lower states has been studied by use of the angular distributions obtained from elastic and inelastic proton-scattering experiments<sup>3,4</sup> and by Coulomb-excitation experiments.<sup>5–10</sup> Recently, the  $\text{Ge}^{73}(n, \gamma)\text{Ge}^{74}$  experiment

performed by Weitkamp *et al.*<sup>11</sup> added many levels above 3 MeV and improved the level-energy definition to 4 keV.

The identification of levels populated in the  $\gamma$ -ray cascades following neutron capture is quite direct when one assumes that all high-energy transitions (6–10 MeV) proceed from the neutron-capture state. Supporting evidence for levels suggested in this way can be found among the low-energy transitions that connect the level in question with lower, established levels. Precise measurements of the level spacings and of the  $\gamma$ -ray energies can confirm or deny level interconnections. Precise measurements of the relative strengths of the level interconnections can, in turn, provide clues to the configuration of the level.

The purpose of this work is to further reduce the uncertainty in the energies of the  $\gamma$  rays emitted in the  $\text{Ge}^{73}(n, \gamma)\text{Ge}^{74}$  reaction and thereby reduce the uncertainties in the level energies. It is also intended to provide the first determination of the absolute intensities of the primary  $\gamma$ -ray transitions from the neutron-capture state and of the secondary transitions between low-lying states in this nucleus. The new information has been used to suggest the spins of three known levels and to introduce four more states below an excitation energy of 3 MeV.

### II. EXPERIMENTAL METHOD

#### Apparatus

The experiments were performed with the internal-target facility developed by the Argonne Physics Division and installed at the CP-5 reactor.<sup>12</sup> The principal  $\gamma$ -ray detection device was a disk-shaped  $\text{Ge}(\text{Li})$  crystal with an active volume of 4 cc and a depletion depth of 0.8 cm. It was operated at liquid-nitrogen temperature and mounted so that the  $\gamma$ -ray beam im-

<sup>†</sup> Work performed under the auspices of the U.S. Atomic Energy Commission. This work is based on a thesis submitted to the Illinois Institute of Technology by A.P.M. in partial fulfillment of the requirements for an M.S. degree.

\* Present address: EG & G Co., 680 Sunset Road, Las Vegas, Nev.

<sup>1</sup> C. Ythier, W. Schoo, B. L. Schrom, H. L. Polak, R. K. Girgis, R. A. Ricci, and R. van Lieshout, *Physica* **25** (1959).

<sup>2</sup> E. Eichler, G. D. O'Kelley, R. L. Robinson, J. A. Marinsky, and N. R. Johnson, *Nucl. Phys.* **35**, 557 (1962).

<sup>3</sup> W. Darcey, in *Comptes Rendus du Congrès International de Physique Nucléaire* (Éditions de Centre National de la Recherche Scientifique, Paris, 1964), Vol. 2, p. 456.

<sup>4</sup> J. K. Dickens, F. G. Perey, and R. J. Silva, Oak Ridge National Laboratory Report No. ORNL-3499, 1963, Vol. 1, p. 30 (unpublished).

<sup>5</sup> F. K. McGowan and P. H. Stelson, *Phys. Rev.* **126**, 257 (1962).

<sup>6</sup> P. H. Stelson and F. K. McGowan, *Nucl. Phys.* **32**, 652 (1962).

<sup>7</sup> K. I. Erokhina and I. Kh. Lemberg, *Izv. Akad. Nauk SSSR, Ser. Fiz.* **26**, 205 (1962) [English transl.: *Bull. Acad. Sci. USSR* **26**, 1009 (1962)].

<sup>8</sup> Yu. P. Gangrskii and I. Kh. Lemberg, *Izv. Akad. Nauk SSSR, Ser. Fiz.* **26**, 1001 (1962) [English transl.: *Bull. Acad. Sci. USSR* **26**, 1009 (1962)].

<sup>9</sup> Yu. P. Gangrskii and I. Kh. Lemberg, *Zh. Eksperim. i Teor. Fiz.* **42**, 1027 (1962) [English transl.: *Soviet Phys.—JETP* **15**, 711 (1962)].

<sup>10</sup> R. L. Robinson, P. H. Stelson, F. K. McGowan, J. L. C. Ford, Jr., and W. T. Milner, Oak Ridge National Laboratory Report No. ORNL-3778, 1964, p. 116 (unpublished).

<sup>11</sup> C. Weitkamp, W. Michaelis, H. Schmidt, and A. Fanger, *Z. Physik* **192**, 423 (1966).

<sup>12</sup> G. E. Thomas, D. E. Blatchley, and L. M. Bollinger, *Nucl. Instr. Methods* **56**, 325 (1967).

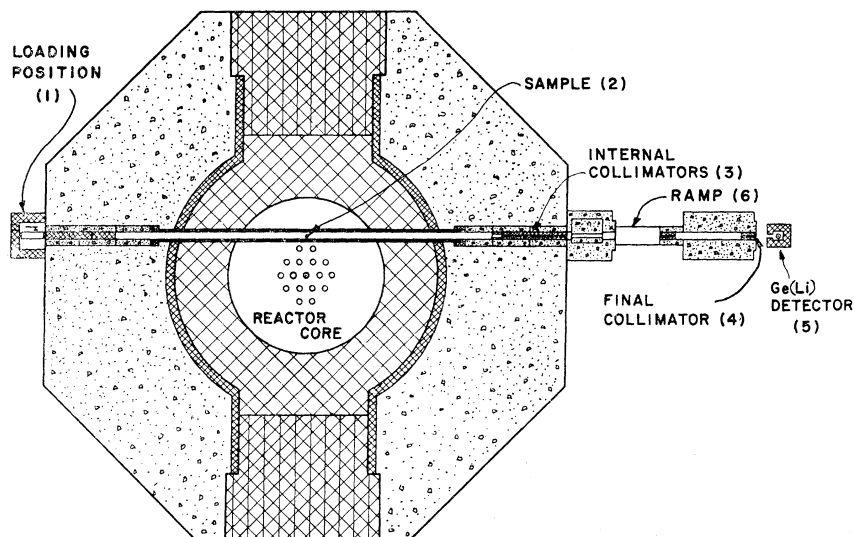


FIG. 1. Experimental arrangement.

pinged upon the edge of the disk. Pulses from this detector were amplified and sent to a 4096-channel analyzer for data storage and punched-tape readout.

Figure 1 indicates the experimental arrangement. The source was contained in a holder made of graphite, secured to a track on a loading device at position (1) and cranked into position (2) where it was subjected to a neutron flux of about  $3 \times 10^{14}$  neutrons/cm<sup>2</sup> sec when the reactor was at full power. The lead collimator (3) within the reactor and the external lead collimator (4) contained in the concrete shield collimated the  $\gamma$ -ray beam from the source before it impinged upon the detector and made it impossible for  $\gamma$  rays from the reactor core and the walls of the beam tube in the high-flux region to reach the Ge(Li) detector directly. This use of a through beam tube and good collimation is the reason for the good signal-to-background ratio observed in this experiment. The  $\gamma$ -ray beam could be further attenuated by placing paraffin or polyethylene blocks on the ramp (6) between the two collimators, or by decreasing the aperture in collimator (4) by inserting a smaller plug, or by using the external controls to move the sample to a position of lower neutron flux.

### Samples

To distinguish between the  $\gamma$ -ray transitions of  $\text{Ge}^{74}$  and transitions belonging to other nuclei, two samples of different enrichments were run. The first was a natural-abundance sample in the form of  $\text{GeO}_2$  powder. With the collimators in place, approximately 9.5 g of the graphite holder and all of the  $\text{GeO}_2$  were visible from the detector position.  $\gamma$  Rays from a chlorine contaminant were evident in the spectra from this source; they probably originated on the relatively large surface area of the graphite holder, where NaCl accumulated from the handling of the sample.

With the second sample, a smaller cylindrical holder was used, and only 2 g of graphite were effectively visible at the detector. The holder enclosed a Ge sample consisting of 0.189 g of metallic powder enriched to 84.1%  $\text{Ge}^{73}$ . The chlorine contaminant had been reduced to approximately 13% of its strength in the natural-abundance source, relative to the intensity of the  $\text{Ge}^{74}$   $\gamma$  rays. Table I presents the absolute and relative cross sections and the isotopic abundances of the germanium isotopes in the two samples.

TABLE I. The isotopic cross section  $\sigma$ , relative abundances  $N_1$  and  $N_2$ , and relative cross sections  $N_1\sigma$  and  $N_2\sigma$  of the mass- $A$  isotopes in the two germanium sources.

$A$	$\sigma$ (b)	$N_1$ (natural) <sup>a</sup>	$N_2$ (enriched) <sup>b</sup>	$N_1\sigma$ (b)	$N_2\sigma$ (b)
70	3.3	0.205	0.024	0.68	0.079
72	0.94	0.274	0.054	0.26	0.051
73	13.7	0.078	0.841	1.06	11.51
74	0.60	0.366	0.071	0.22	0.043
76	0.35	0.078	0.009	0.027	0.0032

<sup>a</sup> Mass of Ge fraction of  $\text{GeO}_2$  sample = 1.43 g.

<sup>b</sup> Mass of  ${}^{73}\text{Ge}$  sample = 0.189 g.

TABLE II. Characteristics of the data runs. The singles type is the full spectrum obtained from the Ge(Li) detector alone; the coincidence type is the spectrum obtained in coincidence with two 0.511-MeV pulses. The linewidths are full widths at half-maximum.

Run No.	Sample	Range (MeV)	Type	Energy calibration (keV/channel)	Duration (h)	Linewidth (keV) at detector energy of		
						0.6 MeV	3.7 MeV	7.7 MeV
1	Natural Ge	0-10	Singles	2.48	18.0	6.6	7.3	8.4
2	Natural Ge	0-10	Coincidence	2.48	22.5	7.2	9.3	11.2
3	Ge <sup>73</sup> enriched	0-10	Singles	2.35	18.5	6.0	7.3	8.0
4	Ge <sup>73</sup> enriched	0-10	Coincidence	2.45	15.3	6.6	11.8	14.1
5	Ge <sup>73</sup> enriched	0-3.7	Singles	0.95	21.8	5.4	14.1	...

### Data

Table II summarizes the characteristics of all the data runs. In all but one data run, the gain of the amplifier was adjusted so that the last channel corresponded to an energy of slightly greater than 10 MeV. This resulted in an energy dispersion of about 2.5 keV/channel in the 4000-channel analyzer. The full linewidth at half-maximum (FWHM) in these runs increased from approximately 6.0 to 8.4 keV over the energy range studied. This variation was due to a baseline drift plus the natural linewidth of the detector. Figure 2 presents the high-energy singles spectrum from the enriched sample.

To spread out the low-energy spectrum of the enriched source, a run with an energy dispersion of 0.95 keV/channel was taken. The thickness of absorber used was made less than in the full-spectrum run in order to increase the counting rate in the region below 2 MeV relative to the rate at higher energies. The linewidth in this case varied from 5.4 keV at 0.6 MeV to 14.1 keV at 3.7 MeV (the upper energy cutoff of the detector). The greater width at higher energies resulted from drifts in the analyzer gain and from pile-up of the detector pulses in the analyzer—a direct consequence of the increased over-all counting rate and the lack of gain stabilization. Part of this data run is presented in Fig. 3(b).

In an auxiliary experiment, illustrated in Fig. 4, two sodium iodide detectors faced the germanium detector at 180° to each other and at 90° to the beam. Pulses from each NaI detector went through an amplifier to an analyzer where a window was set to preferentially accept 0.511-MeV pulses. These pulses then went to a coincidence circuit which gated the germanium detector pulses into the 4096-channel analyzer. With this arrangement, the facility was operated as a true pair spectrometer, counting only those pulses in the germanium detector that were accompanied by two oppositely directed 0.511-MeV annihilation quanta. These runs were used to distinguish the double-escape peaks in the spectra from single-escape and full-energy peaks. The linewidth again suffered from drift of the analyzer gain and from pile-up, since some of the absorber was removed to increase the

over-all counting rate. Figure 3(a) shows the high-energy portion of the coincidence spectrum obtained with the natural-abundance source.

A pulser and a precision digital voltmeter were also used to insert pulses of measured voltage into energy-calibration runs. These runs, which were intended to correct for a nonlinear response of the system, were taken against a short-term Ge<sup>73</sup>(*n*,  $\gamma$ )Ge<sup>74</sup> background so that pulser peaks from a precision pulser could be directly compared with prominent Ge<sup>74</sup>  $\gamma$  rays.

### III. METHOD OF ANALYSIS

#### Energy Calibration

The  $\gamma$  rays used as standards for the energy calibration of the Ge<sup>74</sup> spectrum were the annihilation radiation<sup>13</sup> at 511.006±0.002 keV, the C<sup>12</sup>(*n*,  $\gamma$ )C<sup>13</sup> line<sup>14</sup> at 4946.0±1.0 keV, and the N<sup>14</sup>(*n*,  $\gamma$ )N<sup>15</sup> line<sup>15</sup> at 10 830.0±1.0 keV. Since all but a few of the measured  $\gamma$  rays are within the range defined by these three calibration lines, the need to extrapolate in most cases is obviated. The more recent value of Greenwood<sup>16</sup> for the N<sup>14</sup>(*n*,  $\gamma$ )N<sup>15</sup> line is 10 829.0±0.6 keV. If this number were used in the energy calibration, it would lower the high-energy end of the spectrum by 1 keV. Since this is well within the error of the experiment, no correction has been made. The nitrogen  $\gamma$  rays came from air remaining in the reactor after the source had been inserted and decreased in intensity as the system was flushed with helium. Although this line was weak, it was easily definable by virtue of its isolation as the highest energy  $\gamma$  ray visible in the full-spectrum runs. The carbon line had its origin in the source holder and dominated its region of the spectrum. This was true even with the small holder, although its use reduced the C/Ge<sup>74</sup> ratio of  $\gamma$ -ray intensities to 20% of its former value. The annihilation radiation could be

<sup>13</sup> E. R. Cohen and J. W. M. DuMond, Rev. Mod. Phys. **37**, 537 (1965).

<sup>14</sup> H. E. Jackson, A. I. Namenson, and G. E. Thomas, Phys. Letters **17** (3), 15 (1965).

<sup>15</sup> F. Everling, L. A. König, J. H. E. Mattauch, and A. H. Wapstra, Nucl. Phys. **18**, 529 (1965).

<sup>16</sup> R. C. Greenwood, Phys. Letters **27B**, 274 (1968).

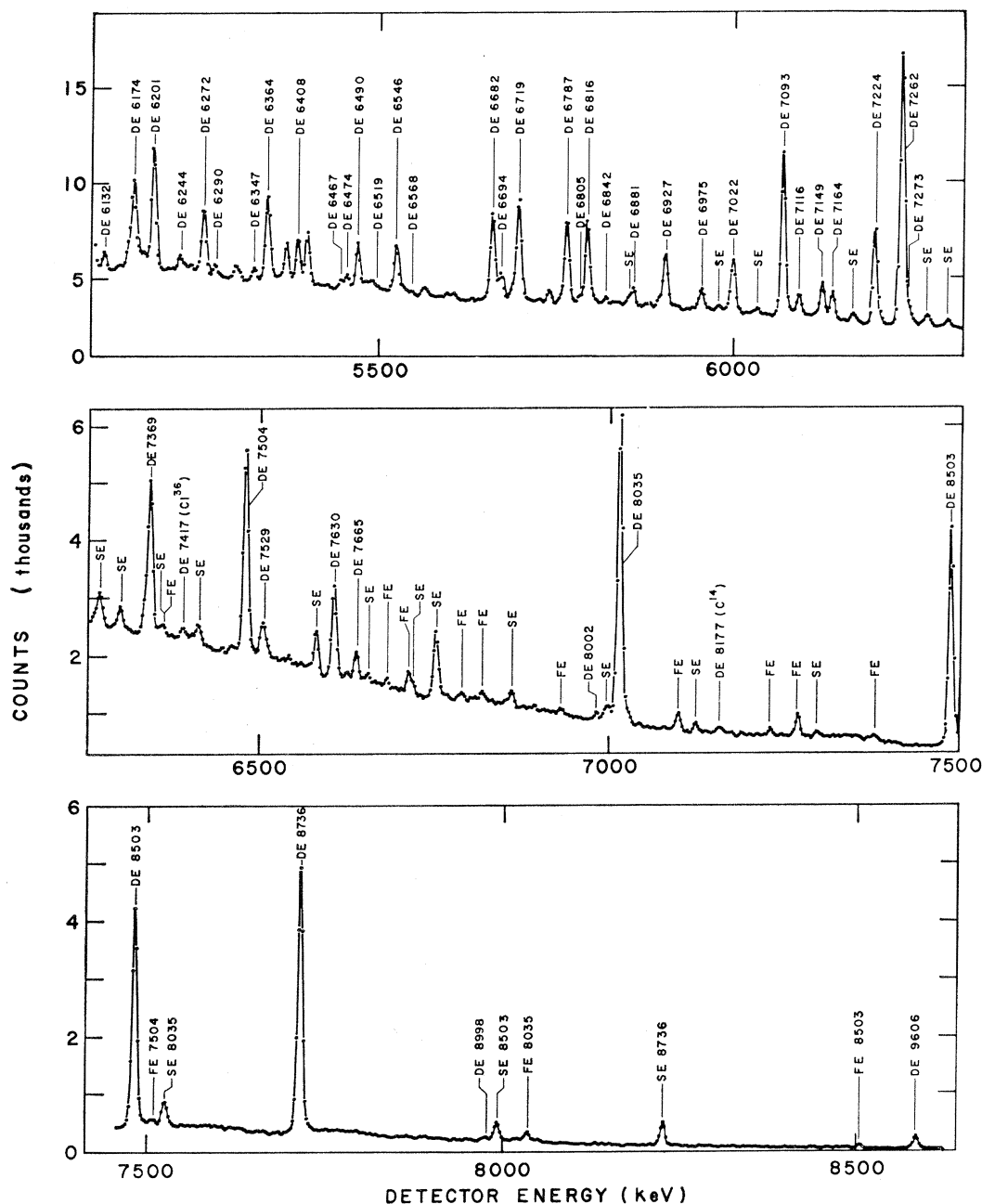


FIG. 2. High-energy singles spectrum from the enriched sample. Double-escape, single-escape, and full-energy peaks are indicated by DE, SE, and FE, respectively. The  $\gamma$ -ray energy in keV follows this label.

produced by any high-energy  $\gamma$  ray (either from the sample or scattered from within the reactor) after pair production and subsequent positron-electron annihilation. It formed a well-resolved line in the low-energy part of the spectrum near the strong 596.3-keV transition from the first  $2^+$  state to the  $0^+$  ground state, and was therefore a convenient calibration line.

These lines were used in conjunction with a curve of pulse height versus channel number in the analyzer.

This curve was obtained as follows: The calibration runs employing the pulser and digital voltmeter provided a set of lines whose voltages had been measured and whose corresponding channel positions in the analyzer were measurable. The pulser positions were determined by fitting a Gaussian shape to the experimental peaks by means of a  $\chi^2$  minimization, with the centroid taken as the peak position. The points on the curve of channel number versus pulser voltage were compared

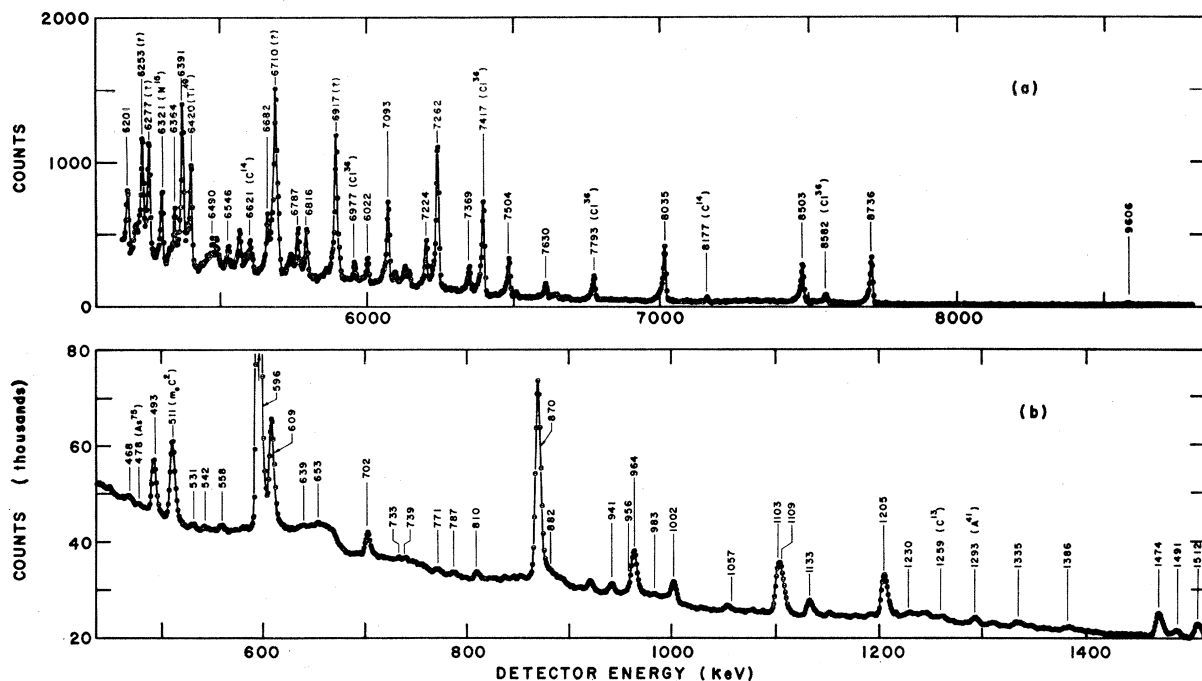


FIG. 3. Spectra from the two samples: (a) the high-energy coincidence spectrum from the natural-abundance sample, and (b) the low-energy singles spectrum from the sample enriched in Ge<sup>73</sup>.  $\gamma$ -ray energies are indicated in keV.  $\gamma$  rays not originating in Ge<sup>74</sup> are labeled either with the nuclide responsible or with a question mark.

with a line by a least-squares minimization procedure. The deviation of pulser points was converted from voltage into energy and plotted as solid points with error bars in Fig. 5. A smooth curve was then drawn through the deviations, and the pulser voltages were changed to fall on the curve (points shown by open squares in Fig. 5). This procedure, which assumes that the peak position is a smooth function of the pulser voltage, is used to reduce the effects of the statistical errors in the location of peak positions and of possible errors in the measurement of the pulser voltages. The dominant linear term is removed to facilitate the plotting and the analysis of the curve, but it does not affect the calibration. This revised set of points provided a response curve (energy versus channel number) for the detector. This curve was translated into a curve of  $\gamma$  energy versus channel number by normalization to the carbon double-escape peak at 4.946 MeV (detector energy 3.924 MeV) and by constraining the curve to pass through the other two calibration points at the  $\gamma$ -ray energies of 0.511 MeV and 9.808 MeV (the double-escape peak of the 10.830-MeV  $\gamma$  ray). The normalization assumes that the energy left in the detector is directly proportional to the pulse height produced. Figure 5 illustrates the deviations from linearity and from a smooth curve as exhibited in one of the three calibration runs used. Good agreement (within  $\pm 0.5$  keV) was obtained between the three calibration runs for the energies of the stronger lines in the spectrum.

A set of the stronger lines in the Ge<sup>74</sup> spectrum also came through in each calibration run, and their energies could be determined directly from the corresponding response curve. This was done by a three-point interpolation between adjusted pulser positions. The channel position of the  $\gamma$  ray, together with the response function, determined the corresponding detector voltage and, by the normalization, the detector energy. Since it was still possible for the detector response to vary statistically between the three normalization points, the detector energy of the set of strong lines was calculated in each of the three calibration runs and the mean value was found. The deviation from the mean for most of the lines was considerably smaller than the uncertainty in the primary calibration lines and constituted only a small fraction of their quoted error. This set of mean values was subsequently used in the long-term run to intercalibrate the lines of smaller intensity by a linear interpolation between the predetermined stronger lines. This procedure assumes that the detector response is linear in the short regions of the spectrum between the strong lines.

The calibration of the high-energy region of the spectrum was checked by comparing the energies of several of the strong lines from the chlorine contaminant with values obtained by Hughes *et al.*<sup>17</sup> for the Cl<sup>35</sup>(n,  $\gamma$ )Cl<sup>36</sup> reaction. Although differences as large as 2.5 keV were

<sup>17</sup> L. B. Hughes, T. J. Kennett, and H. Lycklama, Argonne National Laboratory Report No. ANL-7282, 1968, p. 319 (unpublished).

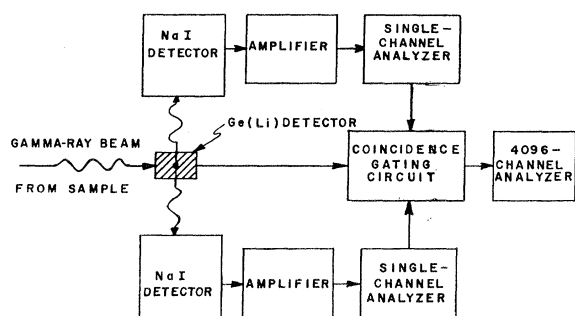


FIG. 4. Schematic diagram of the auxiliary coincidence experiment.

noted in the energy range from 4.9 to 8.6 MeV, the two sets of measurements agreed to within their errors. For these chlorine lines, our values based on the nitrogen and carbon lines were, on the average, 1–2 keV lower than those of Hughes *et al.*<sup>17</sup> After the analysis was completed, new values for the chlorine lines were published by Hughes,<sup>18</sup> which were lower by 1–3 keV than his earlier work<sup>17</sup> and lower, on the average, than our numbers by 1 keV. Since Hughes quotes an error of  $\pm 2$  keV on these values, the agreement is still good.

One line in the low-energy spectrum was independently cross-checked by use of an external  $\text{Co}^{60}$  source. When the  $\text{Co}^{60}$  full-energy lines<sup>19</sup> at  $1173.22 \pm 0.004$  and  $1332.48 \pm 0.05$  keV were superimposed on the  $\text{Ge}^{74}$  spectrum, they bracketed the strong  $\text{Ge}^{74}$  transition at 1.2 MeV. The energy determined by a linear interpolation between the  $\text{Co}^{60}$  lines was  $1204.83 \pm 0.7$  keV, whereas the mean value obtained by use of the pulser calibrations was  $1204.94 \pm 0.9$  keV. This line is of particular importance in the level scheme since it is the direct transition from the second excited state to the ground state. As such, its energy is also equal to the sum of the energies of the transitions from the second state to the first and from the first state to the ground state. These two transitions form a fully resolved doublet whose separation was measured at  $12.3 \pm 0.1$  keV. From this separation and the value  $1204.9 \pm 0.6$  keV for the sum, the energy of the transition from the second excited state to the first is found to be  $608.6 \pm 0.4$  keV and that of the transition from the first to the ground state is  $596.3 \pm 0.4$  keV. The mean value obtained for the latter strictly from the pulser calibration was  $596.7 \pm 0.6$  keV. Both determinations compare well with a recent published value of  $596.0 \pm 0.3$ , also obtained with a  $\text{Ge}(\text{Li})$  detector.<sup>20</sup>

#### Intensity Calibration

Figure 6 shows the relative efficiency of the  $\text{Ge}(\text{Li})$  detector crystal plotted as a function of  $\gamma$ -ray energy. It was obtained with the aid of a number of different

<sup>18</sup> L. B. Hughes, thesis, McMaster University, 1967 (unpublished).

<sup>19</sup> G. Murray, R. L. Graham, and J. S. Geiger, *Nucl. Phys.* **63**, 353 (1965).

<sup>20</sup> R. L. Robinson, P. H. Stelson, F. K. McGowan, J. L. C. Ford, Jr., and W. T. Milner, *Nucl. Phys.* **74**, 1281 (1965).

$\gamma$ -ray sources. For the very low-energy end of the spectrum, a small sample of  $\text{Hf}^{179}$  was irradiated for a short time, and the radioactive decay lines were measured with this  $\text{Ge}(\text{Li})$  detector. The transitions observed are indicated in the level scheme shown in Fig. 7. Since the origin of all activity is the 1.141-MeV level, the absolute intensities must satisfy the relations

$$I_{215} = I_{93} = I_{332} = I_{501} + I_{443}$$

and

$$I_{58} = I_{443}.$$

Let  $I_A$  be the absolute transition intensity of the nucleus,  $I_0$  be the observed  $\gamma$ -ray intensity after passage through the system,  $S$  be the system efficiency for detection of  $\gamma$  rays, and  $\alpha$  be the internal conversion coefficient. Then

$$I_A = I_0 \times (1 + \alpha) / S.$$

The relative detector efficiency is determinable at all of the  $\gamma$  energies in the cascade with the additional assumption that the efficiency at 58 keV is approximately the same as at 93 keV. The internal conversion coefficient  $\alpha$  depends on the multipolarity of the transition.

In the region 0.558–1.660 MeV, a set of strong lines in the  $\text{Cd}^{113}(n, \gamma)\text{Cd}^{114}$  spectrum was used to determine the full-energy-peak efficiency curve. A small sample was placed in the reactor, and the observed intensities were compared with relative intensity measurements of the same  $\gamma$  rays from the bent-crystal spectrometer at the Argonne National Laboratory.<sup>21</sup> The beginning of the double-escape efficiency curve was obtained in this same region with a  $\text{Co}^{60}$  radioactive source. The full-energy and double-escape lines of the 1173.22- and 1332.48-keV  $\gamma$  rays were measured, and the ratio of full-energy intensity to double-escape intensity was used to proceed from the full-energy curve to the double-escape efficiency. One additional point at 1.1 MeV in this region and a set of points at higher energies up to 11 MeV were obtained by calibrating with  $\gamma$ 's from

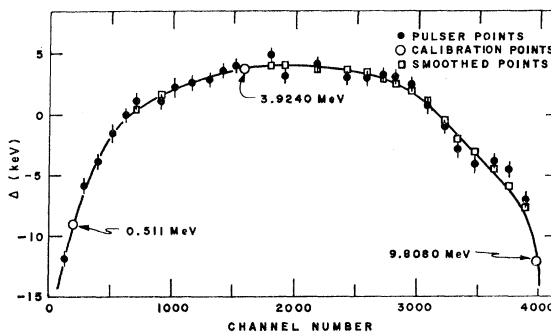


FIG. 5. Deviations  $\Delta$  of the measured energy response of the analyzer from linearity and from a smooth response.

<sup>21</sup> R. K. Smither and D. J. Buss (to be published); R. K. Smither, *Phys. Rev.* **124**, 183 (1961).

beryllium, nitrogen, and carbon sources.<sup>22</sup> In the high-energy region, the full-energy efficiency was tied to the double-escape curve by the full-energy/double-escape intensity ratio observable with the stronger lines in the Cd<sup>113</sup>(n, γ)Cd<sup>114</sup> spectrum.

The experimental curve was checked against a theoretical Monte Carlo calculation by Snow<sup>23</sup> and found to be in fair agreement in its general shape but appreciably different in its absolute values in some regions. In the low-energy region, the full-energy peaks dominate. They result from the combination of a strong photoelectric effect and Compton-scattering events in which both the Compton electron and the γ ray are stopped in the detector. At a γ-ray energy of 2.2 MeV, the pair-production cross section has increased enough to make the double-escape and full-energy efficiencies the same, and it continues to increase with energy as the cross sections for Compton scattering and the photoelectric effect go down. The double-escape efficiency, however, reaches a maximum at about 5 MeV and then drops off as more of the energetic electrons and positrons escape from the germanium detector crystal. A similar decrease in efficiency is present in the full-energy curve because of the escape of high-energy Compton electrons. It should be noted that the effi-

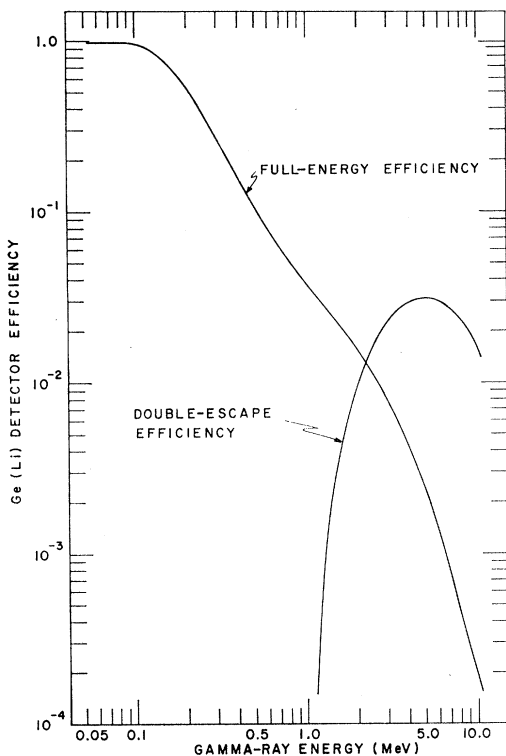


FIG. 6. Efficiency of the Ge(Li) detector crystal.

<sup>22</sup> G. E. Thomas, D. E. Blatchley, and L. M. Bollinger, Nucl. Instr. Methods 56, 325 (1967).

<sup>23</sup> W. J. Snow, Argonne National Laboratory Report No. ANL-7314, 1967 (unpublished).

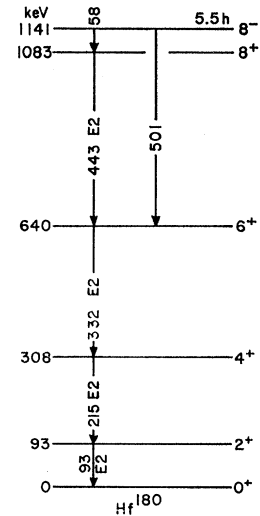


FIG. 7. Decay scheme of the 5.5-h isomeric state in Hf<sup>180</sup>. All energies are given in keV.

ciency curve shown in Fig. 6 is for the bare Ge(Li) detector. In calculating the intensities of the γ rays, it was necessary to correct for their absorption in the sample itself as well as for the absorption in the source holder and in the material between the source and the detector. These corrections are not negligible; they contribute substantially to the errors quoted for the low-energy part of the spectrum.

The two C<sup>12</sup>(n, γ)C<sup>13</sup> γ rays at 4.946 and 3.684 MeV were used as intensity standards within the data runs to normalize the measured peak areas  $A_C$  to the known<sup>24,25</sup> absolute intensities  $I_C=69$  and 31 γ's per 100 neutron captures, respectively, thereby obtaining the normalization constant

$$B = I_C \times F_C / A_C,$$

where  $F_C$  represents the efficiency of the total detector system at each C<sup>13</sup> γ-ray energy. If one used the more recent values of Thomas *et al.*<sup>22</sup> for the absolute intensities of the carbon lines,  $I_\gamma(4946) = 66\%$  and  $I_\gamma(3684) = 34\%$ , one obtains the same value for the coefficient  $B$ , since the sum of their intensities is still 100%. These γ rays originated in the graphite-source holder and the amount of C<sup>12</sup> visible to the detector was calculable from the source-detector configuration. The absolute intensity  $I_G$  of the Ge<sup>74</sup> γ rays was then related to the measured peak areas  $A_G$  by

$$I_G = B(\sigma_C N_C / \sigma_G N_G) A_G / F_G,$$

where  $\sigma_C = 3.3 \pm 0.2$  mb and  $\sigma_G = 13.7 \pm 1.2$  b are the respective neutron-capture cross sections of C<sup>12</sup> and Ge<sup>73</sup>,  $N_G$  is the amount of Ge<sup>73</sup> within the holder,  $N_C$  is the amount of C<sup>12</sup> visible to the detector, and  $F_G$  is the efficiency of the detector system at each Ge<sup>74</sup> γ-ray

<sup>24</sup> L. V. Groschev, A. M. Demidov, V. N. Lutsenko, and V. I. Pelekhov, *Atlas of γ-Ray Spectra from Radiative Capture of Thermal Neutrons* (Oxford University Press, London, 1959).

<sup>25</sup> L. von Jarczyk, J. Lang, R. Muller, and W. Wolfli, *Helv. Phys. Acta* 34, 483 (1961).

TABLE III. Low-energy  $\gamma$  rays from the reaction  $\text{Ge}^{73}(n, \gamma)\text{Ge}^{74}$ .

Present work (keV)	$E_{\gamma} \pm \Delta E_{\gamma}$ Weitkamp <i>et al.</i> <sup>a</sup> (keV)	Intensity <sup>b</sup> $I_{\gamma} \pm \Delta I_{\gamma}$ ( $\gamma^2/\text{s}/100$ neutron captures)	In level scheme	Remarks
	235 $\pm$ 5	<0.1		
289.2 $\pm$ 2.5	288 $\pm$ 4	0.40 $\pm$ 0.12		
	315 $\pm$ 4	$\leq$ 0.13		c
468.4 $\pm$ 1.2	468 $\pm$ 3	0.73 $\pm$ 0.11	Yes	13% DE 1491 <sup>d</sup>
493.0 $\pm$ 0.8	493 $\pm$ 2	5.36 $\pm$ 0.59	?	
530.9 $\pm$ 1.1	532 $\pm$ 2	0.39 $\pm$ 0.09	Yes	
542.3 $\pm$ 1.4	544 $\pm$ 3	0.20 $\pm$ 0.09		
558.4 $\pm$ 1.4	559 $\pm$ 3	0.42 $\pm$ 0.10		
596.3 $\pm$ 0.4	597 $\pm$ 1	49.9 $\pm$ 5.0	Yes	
608.6 $\pm$ 0.4	609 $\pm$ 1	12.2 $\pm$ 1.3	Yes	
638.6 $\pm$ 1.2		0.30 $\pm$ 0.10		
653.4 $\pm$ 1.4		0.35 $\pm$ 0.10		
702.2 $\pm$ 0.8	703 $\pm$ 2	3.15 $\pm$ 0.34	Yes	
732.6 $\pm$ 1.2		0.20 $\pm$ 0.09	Yes	c
738.8 $\pm$ 1.2	740 $\pm$ 3	0.33 $\pm$ 0.09	Yes	c
771.2 $\pm$ 1.2	772 $\pm$ 2	0.70 $\pm$ 0.12	Yes	
787.0 $\pm$ 1.2	788 $\pm$ 3	0.48 $\pm$ 0.10		27% DE 1811
809.8 $\pm$ 0.8	810 $\pm$ 3	0.61 $\pm$ 0.10	Yes	10% DE 1833
869.9 $\pm$ 0.8	869 $\pm$ 1	26.8 $\pm$ 2.7	Yes	
882.2 $\pm$ 1.2		$\leq$ 1.03 $\pm$ 0.12		Near 870-keV line and Compton edge of 1103-keV line
	920 $\pm$ 2			100% DE 1943 <sup>e</sup>
941.4 $\pm$ 0.8	940 $\pm$ 2	1.30 $\pm$ 0.14		
956.4 $\pm$ 1.2	953 $\pm$ 3	0.43 $\pm$ 0.09		
963.5 $\pm$ 0.8	963 $\pm$ 1	6.07 $\pm$ 0.65	Yes	
982.8 $\pm$ 1.2		0.10 $\pm$ 0.07		c
1001.7 $\pm$ 0.8	1000 $\pm$ 2	1.80 $\pm$ 0.19	?	
1057.2 $\pm$ 1.2	1057 $\pm$ 3	0.21 $\pm$ 0.05		
1103.4 $\pm$ 0.9	1103 $\pm$ 2	8.95 $\pm$ 0.90	Yes	Close doublet
1108.9 $\pm$ 1.2		2.05 $\pm$ 0.21	Yes	
1132.8 $\pm$ 0.8	1132 $\pm$ 3	2.23 $\pm$ 0.24	Yes	
1204.9 $\pm$ 0.6	1208 $\pm$ 5	6.34 $\pm$ 0.63	Yes	
1229.9 $\pm$ 1.2	1232 $\pm$ 5	0.72 $\pm$ 0.10	Yes(2)	Possible doublet 100% DE 2318, FE 1293 (A <sup>41</sup> )
	1295 $\pm$ 4			
1335.3 $\pm$ 1.6	1338 $\pm$ 4	0.51 $\pm$ 0.09	Yes	43% DE 2357
1385.9 $\pm$ 1.2	1390 $\pm$ 5	0.81 $\pm$ 0.11		
	1403 $\pm$ 5	<0.15		Possible Compton edge of 1620- keV line
	1445 $\pm$ 7			100% DE 2473
	1460 $\pm$ 7			
1473.5 $\pm$ 0.9	1478 $\pm$ 3	3.71 $\pm$ 0.30	Yes	
1490.9 $\pm$ 1.2	1495 $\pm$ 4	0.88 $\pm$ 0.11	Yes	17% DE 2513
1511.8 $\pm$ 1.2	1513 $\pm$ 4	1.67 $\pm$ 0.18	Yes	23% DE 2534



TABLE III (Continued)

Present work (keV)	$E_\gamma \pm \Delta E_\gamma$ Weitkamp <i>et al.</i> <sup>a</sup> (keV)	Intensity <sup>b</sup> $I_\gamma \pm \Delta I_\gamma$ ( $\gamma$ 's/100 neutron captures)	In level scheme	Remarks
1577.2±1.2	1580±7	0.59±0.09		
1604.3±2.2	1605±7	0.11±0.05	Yes	
1621.1±1.2	1621±7	0.74±0.10		
1635.8±1.7	1633±7	1.07±0.13		
1643.3±1.7	1650±7	0.75±0.10		
1678.7±1.7	1680±7	0.56±0.09		
1701.1±2.1	1697±7	0.09±0.04		
1714.0±2.1	1720±7	0.40±0.16		c
	1742±7			100% DE 2771
1757.6±2.1		0.20±0.07		
	1768±6			100% DE 2788
1780.2±2.1		0.61±0.07		
1811.3±1.6	1810±7	0.34±0.11		52% DE 2833
1832.6±1.2	1835±7	0.33±0.08		
1845.8±1.2		0.61±0.10		
1876.0±1.2		0.28±0.08		
1914.2±2.1		0.27±0.08		
	1933±7			100% DE 2054
1943.4±1.0	1948±5	2.01±0.25	Yes	
	1965±7			100% DE 2979
2016.8±1.3		0.53±0.09		On Compton edge of 1205-keV line
2040.3±2.1		≤0.1		
2075.3±1.3	2072±5	0.91±0.12	Yes	
2099.2±1.3	2100±10	0.27±0.10	Yes	c
2155.4±3.0	2148±10	≤0.2		c
2174.0±1.3		0.35±0.10		c
2187.2±2.2	2190±10	≤0.2		c
2200.0±1.3		0.21±0.09	Yes	c
2214.2±1.3		0.37±0.09		
2236.7±3.0		≤0.4	Yes	c
2266.1±1.3	2265±7	0.71±0.10		Possible doublet
2282.0±3.0	2280±7	≤0.24		
2317.7±2.2	2318±7	0.35±0.08		Near FE 1293 (A <sup>41</sup> ), c
2332.4±1.3	2337±7	0.45±0.08	Yes	
2357.3±1.6	2357±7	0.37±0.08		57% FE 1335
2368.8±1.3		0.36±0.08		
2389.6±3.0	2395±10	≤0.2		c
	2416±7	<0.1		
2455.7±2.2	2451±7	0.21±0.06		c
2472.7±2.2	2466±7	0.15±0.06		c
	2483±7	<0.1		

TABLE III (Continued)

Present work (keV)	$E_{\gamma} \pm \Delta E_{\gamma}$ Weitkamp <i>et al.</i> <sup>a</sup> (keV)	Intensity <sup>b</sup> $I_{\gamma} \pm \Delta I_{\gamma}$ ( $\gamma$ 's/100 neutron captures)	In level scheme	Remarks
2512.9±1.3		0.15±0.06		
2533.8±1.3		0.39±0.08	c	
2569.9±1.6		0.23±0.07		Possible doublet
2585.1±1.6		0.28±0.07		
2621.8±2.2	2655±10	0.08±0.04		100% FE 1635
2693.1±1.3	2690±10	0.41±0.06		
2700.7±1.7	2710±10	0.36±0.06		
2744.6±2.2		0.22±0.05		On Compton edge of 1943-keV line
2755.1±2.2	2757±10	0.13±0.05		
2771.1±2.2		0.10±0.05		
2788.1±1.3	2793±10	0.61±0.07		
2833.3±1.6		0.21±0.06		48% FE 1811
	2852±10	<0.1		
	2868±10	<0.1		
2880.6±1.3		0.33±0.05		
2909.4±2.2	2900±10	0.12±0.04		
2953.6±2.2		0.11±0.04		
2978.6±2.2		0.10±0.04	c	

<sup>a</sup> Reference 11.

<sup>b</sup> Present work. The error quoted for a  $\gamma$ -ray intensity is relative to other  $\text{Ge}^{74}$   $\gamma$  rays in the spectrum. The error on the absolute intensity requires the vector addition of an additional 17% of the quoted intensity.

<sup>c</sup> Questionable isotopic assignment.

<sup>d</sup> 13% DE 1491 means that 13% of the counting rate at the listed  $\gamma$ -ray energy originates in the double-escape peak (DE) of the 1491-keV  $\gamma$  ray.

This counting rate was subtracted off before the intensity of the listed  $\gamma$  ray was calculated. SE refers to a single-escape peak and FE to a full-energy peak in subsequent references.

<sup>e</sup> 100% DE 1943 means that all of the counting rate at a detector energy of 920-keV was interpreted as originating from the double-escape peak of the 1943-keV  $\gamma$  ray, and not from a full-energy peak at 920 keV.

energy. For additional details concerning the intensity calculations, see the discussion by Magruder.<sup>26</sup>

#### $\gamma$ -Ray Identification

In the region of the spectrum from 6 to 10 MeV, the double-escape character of peaks in the spectrum was established in 36 out of 47 cases by the coincidence run. In this energy range, the double-escape peaks were more than 10 times as large as the single-escape or full-energy peaks. This fact was used to identify weak double-escape peaks, since each single-escape and full-energy peak had to have a much stronger double-escape peak lying, respectively, 0.511 and 1.022 MeV lower in energy. The intensity of each double-escape peak so identified was checked in the singles run and corrected for any contributions from single-escape and full-energy peaks of other  $\gamma$  rays.

After the double-escape character of the peak was established, its intensity from the enriched source was

compared with the intensity from the natural-abundance source in the full-spectrum runs. Absorption effects were similar in the two runs in this energy region so the directly observed intensities could be used for comparison purposes. Transitions from the  $\text{Ge}^{73}(n, \gamma)\text{Ge}^{74}$  reaction were identified by the ratio  $R=0.65 \pm 0.15$  of the enriched-sample intensity to the natural-sample intensity.  $\gamma$  rays from reactions other than  $\text{Ge}^{73}(n, \gamma)\text{Ge}^{74}$  were also observed. They were identified first by the different ratio of the enriched-sample intensity to the natural-sample intensity which they exhibited. The energies of these lines were then compared with the energies of  $\gamma$  rays from contaminants which have been observed previously in  $(n, \gamma)$  spectra obtained with this system.<sup>27</sup> They were also compared with the most likely  $\gamma$  rays from the capture states of other germanium isotopes.<sup>28</sup> Assignments to particular reactions were based on the agreement in

<sup>27</sup> G. Thomas (private communication).

<sup>28</sup> Nuclear Data Sheets, compiled by K. Way *et al.* (Printing and Publishing Office, National Academy of Sciences—National Research Council, Washington, D.C. 20025).

<sup>26</sup> A. P. Magruder, thesis, Illinois Institute of Technology, 1968 (unpublished).

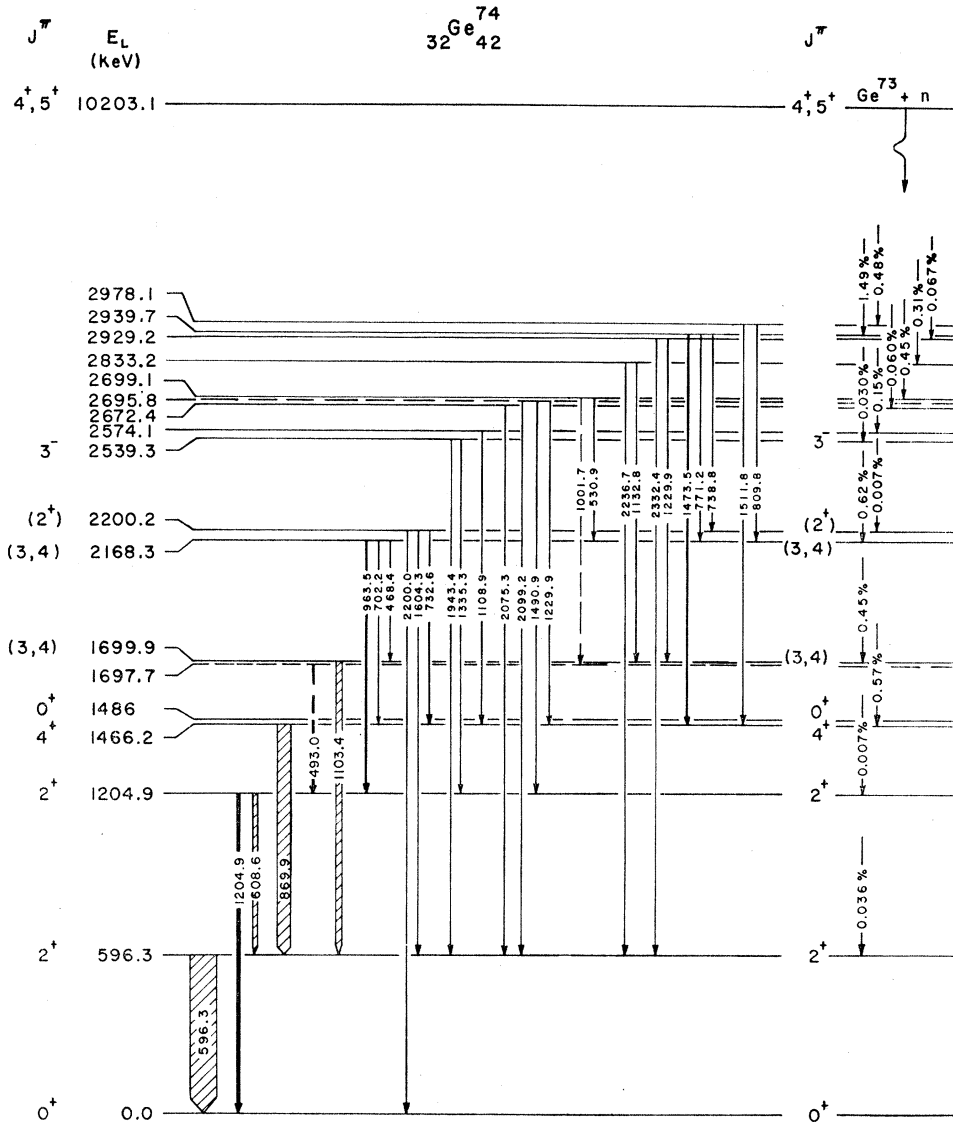


FIG. 8. Energy-level scheme of  $Ge^{74}$ . The intensities of the direct transitions from the neutron-capture state are shown on the right. A spin and parity in parentheses is based on the strength of the direct transition and on the decay of the level. The dashed lines indicate uncertainty in their position and are discussed in the text. All energies are in keV.

the energy values. Some of these  $\gamma$  rays are indicated in Figs. 2 and 3.

In the low-energy region, both double-escape and full-energy peaks were considered. Of the 82 identified lines below  $E_\gamma = 3$  MeV, 44 were substantiated as double-escape peaks by the coincidence run with the enriched sample. In a few cases, the coincidence run was the only evidence for a line because of complications (e.g., full-energy peaks or Compton edges) in the singles spectrum. In general, full-energy peaks were used for energy and intensity measurements below 1.94 MeV, while double-escape peaks were used above.

The effect of using less polyethylene absorber with the enriched sample than with the natural sample could be seen in the low-energy region. Full-energy peaks could be distinguished from double-escape peaks at the same detector energies by use of the ratio of

enriched-sample to natural-sample intensities. This ratio was distinctly larger for full-energy than for double-escape peaks, ranging from four times as large at  $E = 0.9$  MeV to twice as large at 1.6 MeV. This is because full-energy peaks are 1.022 MeV lower on the absorption curve than double-escape peaks at the same detector energy. Some full-energy peaks were also suggested by the observation that the intensity in the coincidence run did not account for all the intensity of the peak in the singles run.

Contaminants in the low-energy region were also identified by their energies and the ratios of their intensities in spectra obtained with the enriched and natural samples. However, the  $\gamma$ -ray intensities in the low-energy region were severely attenuated, and many lines in the data from one sample could not be seen in the data from the other. In these cases the counting

TABLE IV. High-energy  $\gamma$  rays from the reaction  $\text{Ge}^{73}(n, \gamma)\text{Ge}^{74}$ .  $\gamma$  intensities and level energies are from this work.

Present work (keV)	$E_\gamma \pm \Delta E_\gamma$ Weitkamp <i>et al.</i> <sup>a</sup> (keV)	Intensity <sup>b</sup> $I_\gamma \pm \Delta I_\gamma$ ( $\gamma$ 's/100 neutron captures)	Level populated $E_L \pm \Delta E_L$ (keV)	Remarks
9606.0 $\pm$ 1.7	9598 $\pm$ 15	0.036 $\pm$ 0.004	596.3 $\pm$ 0.4	
8997.7 $\pm$ 1.4	9001 $\pm$ 12	0.007 $\pm$ 0.002	1204.9 $\pm$ 0.6	
8736.4 $\pm$ 1.3	8738 $\pm$ 10	0.574 $\pm$ 0.058	1466.2 $\pm$ 0.6	
8502.5 $\pm$ 1.3	8500 $\pm$ 10	0.451 $\pm$ 0.046	1699.9 $\pm$ 0.6	
8034.5 $\pm$ 1.4	8032 $\pm$ 10	0.624 $\pm$ 0.063	2168.3 $\pm$ 0.5	
8002.2 $\pm$ 2.2		0.007 $\pm$ 0.003	2200.2 $\pm$ 0.9	36% FE 6975 <sup>c</sup>
7664.9 $\pm$ 1.8		0.030 $\pm$ 0.005	2539.3 $\pm$ 0.6	32% SE 7149
7629.5 $\pm$ 1.5		0.154 $\pm$ 0.017	2574.1 $\pm$ 0.8	
7528.9 $\pm$ 1.8		0.060 $\pm$ 0.009	2672.4 $\pm$ 0.7	30% SE 7022
7504.1 $\pm$ 1.4	7504 $\pm$ 8	0.453 $\pm$ 0.046	2699.1 $\pm$ 0.7	
7369.1 $\pm$ 1.4	7363 $\pm$ 8	0.311 $\pm$ 0.032	2833.2 $\pm$ 0.5	
7273.0 $\pm$ 2.8		0.067 $\pm$ 0.009	2929.2 $\pm$ 0.8	
7262.3 $\pm$ 1.3	7259 $\pm$ 8	1.49 $\pm$ 0.15	2939.7 $\pm$ 0.5	
7224.2 $\pm$ 1.3	7225 $\pm$ 8	0.481 $\pm$ 0.049	2978.1 $\pm$ 0.5	11% SE 6719
7163.6 $\pm$ 1.4	7164 $\pm$ 10	0.128 $\pm$ 0.014		
7149.4 $\pm$ 1.4	7147 $\pm$ 10	0.189 $\pm$ 0.020		
7116.4 $\pm$ 1.4		0.101 $\pm$ 0.012		
7093.3 $\pm$ 1.3	7091 $\pm$ 8	0.834 $\pm$ 0.084		
7021.8 $\pm$ 1.2	7022 $\pm$ 8	0.288 $\pm$ 0.030		
6975.4 $\pm$ 2.2	6977 $\pm$ 12	0.130 $\pm$ 0.015		Near DE 6977 (Cl <sup>36</sup> )
6926.7 $\pm$ 1.4	6926 $\pm$ 8	0.278 $\pm$ 0.029		
6881.2 $\pm$ 1.6		0.069 $\pm$ 0.010		
6841.6 $\pm$ 2.2		0.028 $\pm$ 0.006		
6816.0 $\pm$ 1.3	6814 $\pm$ 10	0.432 $\pm$ 0.044		
6804.8 $\pm$ 1.7		0.035 $\pm$ 0.009		
6787.1 $\pm$ 1.3	6785 $\pm$ 10	0.428 $\pm$ 0.044		
6719.4 $\pm$ 1.4	6717 $\pm$ 8	0.585 $\pm$ 0.059		
6694.4 $\pm$ 2.8		0.130 $\pm$ 0.015		
6682.1 $\pm$ 1.2	6683 $\pm$ 8	0.478 $\pm$ 0.044		
	6624 $\pm$ 10			Masked by SE 6118, SE6111, DE 6621 (all Cl <sup>36</sup> )
	6590 $\pm$ 12			
6568.1 $\pm$ 2.2		0.013 $\pm$ 0.006		
6545.5 $\pm$ 1.3	6547 $\pm$ 10	0.246 $\pm$ 0.028		
6518.5 $\pm$ 3.0	6522 $\pm$ 12	0.032 $\pm$ 0.007		
6490.3 $\pm$ 1.5	6488 $\pm$ 8	0.218 $\pm$ 0.024		
6474.2 $\pm$ 1.5		0.046 $\pm$ 0.009		32% SE 5960
6466.9 $\pm$ 2.8	6467 $\pm$ 12	0.040 $\pm$ 0.008		
	6424 $\pm$ 12			
6407.7 $\pm$ 1.5	6404 $\pm$ 12	0.232 $\pm$ 0.025		
6363.7 $\pm$ 1.2	6365 $\pm$ 8	0.548 $\pm$ 0.056		
6347.3 $\pm$ 2.3		0.042 $\pm$ 0.010		31% SE 5836
6280.6 $\pm$ 2.2		0.047 $\pm$ 0.009		

TABLE IV (Continued)

Present work (keV)	$E_\gamma \pm \Delta E_\gamma$ Weitkamp <i>et al.</i> <sup>a</sup> (keV)	Intensity <sup>b</sup> $I_\gamma \pm \Delta I_\gamma$ (γ's/100 neutron captures)	Level populated $E_L \pm \Delta E_L$ (keV)	Remarks
6272.1±1.7	6272±8	0.310±0.034		
6243.5±1.5	6242±12	0.066±0.010		
6201.2±1.2	6202±8	0.570±0.060		
6188.7±2.5		0.097±0.012		
6182.5±2.5		0.067±0.012		30% SE 5661
6173.8±2.2	6175±8	0.368±0.038		
6166.3±2.5		0.106±0.013		
6131.6±2.2		0.062±0.011		12% SE 5120

<sup>a</sup> Reference 11.

<sup>b</sup> Present work. The error quoted for a γ-ray intensity is relative to other Ge<sup>74</sup> γ rays in the spectrum. The error on the absolute intensity requires the vector addition of an additional 17% of the quoted intensity.

<sup>c</sup> 36% FE 6975 means 36% of the counting rate observed in the data

at the listed γ-ray energy originates in the full-energy (FE) peak of the 6975-keV γ ray. This intensity was subtracted off before the intensity of the listed γ ray was calculated. SE refers to a single-escape peak and DE to a double-escape peak in subsequent references.

statistics were used as upper limits for a determination of the intensity ratio between the enriched and natural samples. The background here was also more difficult to judge than in the high-energy region because of a higher density of lines and the presence of prominent Compton edges. In this region, therefore, a larger error in the background led to a larger error in the intensities. These complications and the fact that the full-energy and double-escape peaks exhibited different energy-dependent ratios made the isotopic and contaminant identification much more subject to error in many cases. γ rays that appeared strongly in both the enriched-sample and natural-sample runs, and yet had the wrong intensity ratio, were interpreted as fortuitous agreements between a Ge<sup>74</sup> line in the enriched run and an impurity line in the natural run. They are listed as lines of questionable isotopic assignments.

#### IV. RESULTS AND ERRORS

The energies and intensities of the γ rays identified as belonging to the reaction Ge<sup>73</sup>(n, γ)Ge<sup>74</sup> are presented in Tables III and IV. The energies in column 1 of Tables III and IV can be compared with the results of the other (n, γ) investigation of this nucleus,<sup>11</sup> which are tabulated in column 2. The quoted errors on the energies are composed of (1) a 0.6-keV error due to the possible variation in the pulser calibration curve, (2) the errors Δ<sub>s</sub> in the peak position relative to the secondary calibration lines, and (3) a systematic error Δ<sub>c</sub> from the error in the primary calibration lines. The errors are added vectorially so that the value (in keV) is

$$\Delta_{\text{tot}} = [(0.6)^2 + \Delta_s^2]^{1/2}.$$

In the low-energy region, the systematic error due to the calibration lines was 0.15 keV at 511.0 keV and 1 keV at 3924.0 keV. A linear interpolation between these values was used to estimate the contribution to

the total error at intermediate points. In the high-energy region, the error due to the calibration lines was 1.0 keV, since both the 4936-keV and 10 830-keV γ rays carried 1-keV errors.<sup>14</sup> Recent measurements of the nitrogen calibration line<sup>16</sup> at 10.8 MeV suggest that the value used was 1 keV too high; this implies that the γ energies in Table IV may also be too high by 1 keV in the upper end of the spectrum.

There are three separate contributions to errors in the absolute γ-ray intensities. The first, fixed at 11%, is contained in the proportionality factor between the observed peak areas and the absolute intensity of the carbon lines. It is determined from the combination of errors in the detector efficiency, in the carbon-line intensities, and in the mean value of the constant determined therefrom. The second contribution arises in the conversion from neutron captures in carbon to neutron captures in germanium. This large uncertainty of 17% is due to the uncertainty in the neutron-capture cross sections and to the uncertainty in the amount of the carbon holder that is effective as a source for the Ge(Li) detector. The third contribution is the error in the actual measurement of the raw intensity; in this analysis it is the error in the area under the γ-ray peak. The combination of the first two contributions places a lower limit of 20% on the errors associated with absolute intensities. Relative intensities, however, are completely unaffected by the second error listed above and are affected by only one part of the first, namely, the error in the relative detector efficiency. Since relative intensities are useful in descriptions of the depopulation of excited nuclear states, their errors are more pertinent than the errors in the absolute intensities. Therefore, the errors quoted in Tables III and IV, column 3 are composed of a 10% relative efficiency error vectorially added to the error in the raw intensity measurement. The error on the

TABLE V. The energy levels of  $\text{Ge}^{74}$  below an excitation energy of 3 MeV. The spin and parity assignments shown in parentheses are those suggested by the  $(n, \gamma)$  data.

Excitation energy (keV)	Error (keV)	Spin and parity
0.0	0.0	$0^+$
596.3	0.4	$2^+$
1204.9	0.6	$2^+$
1466.2	0.6	$4^+$
1486.0 <sup>a</sup>	7.0 <sup>a</sup>	$0^+$
1697.7	1.0	
1699.9	0.6	$(3^{\pm}, 4^+)$
2168.3	0.5	$(3^{\pm}, 4^+)$
2200.2	0.9	$(2^+)$
2539.3	0.6	$3^-$
2574.1	0.8	$(6^+)$
2672.4	0.7	
2695.8	0.7	
2699.1	0.7	
2833.2	0.5	
2929.2	0.8	
2939.7	0.5	
2978.1	0.5	

<sup>a</sup> From Ref. 3.

absolute intensity would require the vector addition of an additional 17%.

Column 4 in Table III indicates which  $\gamma$  rays have been incorporated in the level scheme. The corresponding column in Table IV lists the level populated by the high-energy  $\gamma$  ray. The final column in each of the two tables is intended to indicate the complications involved in defining the  $\gamma$  ray and to explain some differences between the interpretation of the spectrum in Ref. 11 and in this work.

The region of the spectrum from 3 to 6 MeV consisted of many closely spaced, low-intensity  $\gamma$  rays. Although many levels above 3 MeV were indicated by the high-energy lines, they could not be reliably verified by connections to lower levels.

## V. DISCUSSION OF THE LEVEL SCHEME

The energy levels of  $\text{Ge}^{74}$ , as indicated by this and other investigations, are shown in Fig. 8 and tabulated in Table V. The level energies are based on the combination of low-energy  $\gamma$  rays between lower levels and on the relative separation of the high-energy  $\gamma$  rays. Direct transitions from the capture state are shown on the far right of Fig. 8 by arrowheads and intensity values. The secondary low-energy transitions are drawn

between levels with a linewidth proportional to the  $\gamma$ -ray intensity. The spin and parity of the level, to the left of the level energy, are in parentheses when they are based solely on the  $\gamma$ -ray intensities that feed and deplete the level.

The level energy of the neutron-capture state was determined from measurements of the direct transitions to, and the  $\gamma$ -ray cascades from, the first three excited states of  $\text{Ge}^{74}$ . This is shown in Table VI. The coupling of a spin- $\frac{1}{2}$  (*s*-wave) neutron to the  $J^{\pi}=\frac{9}{2}^+$  ground state<sup>29</sup> of  $\text{Ge}^{73}$  restricts the spin and parity of the capture state to the values  $J^{\pi}=4^+$  or  $5^+$ .

### Direct $E2$ Transitions

Restricting the spin and parity of the capture state to  $J^{\pi}=4^+$  or  $5^+$  also limits the possible spins and parities of the levels that can be populated directly from the capture state with a measurable intensity. The range of  $J^{\pi}$  values reached through  $E1$  transitions is  $3^- \leq J^{\pi} \leq 6^-$ ; through  $M1$  transitions,  $3^+ \leq J^{\pi} \leq 6^+$ ; and through  $E2$  transitions,  $2^+ \leq J^{\pi} \leq 7^+$ . For higher multipoles, the transition probability is several orders of magnitude smaller than it is for  $M1$  transitions. As a result, strong direct transitions are assumed to be  $M1$  or  $E1$ , and the lowest spin possible for the lower state in question is  $J=3$ . Weak direct transitions may be  $E2$ , and the lowest spin possible is  $J^{\pi}=2^+$ .

Evidence supporting these assumptions was found in the relative strength of the direct transitions to the first three excited states. The spins and parities of these states have been established by Coulomb excitation<sup>6-10</sup> and by scattering experiments.<sup>3,4</sup> The 596.3- and 1204.9-keV levels are  $2^+$  states and, on the above assumptions, the lowest multipolarity possible for transitions direct from the capture state is  $E2$ . The 1466.2-keV level is a  $4^+$  state and the multipolarity of a direct transition is most likely to be  $M1$ .

The intensities of the transitions from the capture state to the levels at 596.3, 1204.9, and 1466.2 keV were experimentally in the ratio 5:1:82. Single-particle estimates<sup>30</sup> predict 1.4:1:14 on the assumption of  $E2$  multipolarity for the transitions to the lower two states and pure  $M1$  multipolarity for the transition to the 1466.2-keV state. Consequently, the transitions to the first two  $2^+$  states at 596.3 and 1204.9 keV (with  $\gamma$ -ray energies of 9606.0 and 8997.7 keV) are, if anything, somewhat weaker than expected from the single-particle estimates but are certainly in approximate agreement with the intensity expected for  $E2$  transitions. We conclude that they are likely to be  $E2$  transitions and that the other weak direct transitions may also be  $E2$ .

An alternative explanation of the weak direct tran-

<sup>29</sup> C. H. Townes, J. M. Mags, and B. P. Dailey, Phys. Rev. **76**, 700 (1949).

<sup>30</sup> S. A. Moszkowski, in *Alpha-, Beta-, and Gamma-Ray Spectroscopy*, edited by K. Siegbahn (North-Holland Publishing Co., Amsterdam, 1965), Chap. XIII.

sitions to  $J^\pi=2^+$  states is  $p$ -wave neutron capture. The angular momentum of the compound state formed by a  $p$ -wave neutron and the  $J^\pi=\frac{3}{2}^+$  ground state of Ge<sup>73</sup> would then be limited to  $3^- \leq J^\pi \leq 6^-$  and electric-dipole transitions to  $2^+$  states would be possible. However, no  $p$ -wave resonances were observed in germanium in a recent experiment at Argonne.<sup>31</sup>

### Individual Levels

#### 1. Ground State

The ground state of Ge<sup>74</sup> has a measured<sup>28</sup> spin and parity  $0^+$ , as is expected for an even- $Z$ -even- $N$  nucleus. The neutron-capture state is  $4^+$  or  $5^+$ , so that no primary  $\gamma$  transition from the neutron-capture state to the ground state is expected or observed [ $I_\gamma(\text{G.S.}) < 0.001\%$ ].

#### 2. 596.3-keV Level

The energy of the 596.3-keV state was determined by the energy of the ground-state transition,  $596.3 \pm 0.4$  keV. The calibration, described in Sec. III, is based on a measurement of the separation between the 596-keV and the 609-keV  $\gamma$  rays and on the calibration of the 1205-keV line in Ge<sup>74</sup> with two Co<sup>60</sup>  $\gamma$ -ray standards.

This level has been established as a  $2^+$  state from measurements of the angular distribution of scattered protons and from Coulomb-excitation measurements.<sup>3-10</sup> It is directly populated from the capture state by a transition whose strength is consistent with  $E2$  multipolarity.

#### 3. 1204.9-keV Level

The energy of the 1204.9-keV level is based on the calibration of the  $\gamma$  at  $1204.9 \pm 0.6$  keV by the method described in Sec. III.

The separation of 608.6 keV between the 596.3- and 1204.9-keV levels is in very good agreement with the independent value of 608.7 keV obtained from the high-energy  $\gamma$  rays (Table IV).

The 1204.9-keV level is also  $2^{+3-10}$  and is populated from the capture state by a transition whose strength is consistent with  $E2$  multipolarity. The observed  $\gamma$ -ray branching ratio  $I_\gamma(609)/I_\gamma(1205)$  is in good agreement with the  $\beta$ -decay results.<sup>2,32-34</sup> (Table VII gives comparison of the four experimental values for this ratio.) The 608.6-keV transition ( $2^{+'} \rightarrow 2^+$ ) is 90%  $E2$  and 10%  $M1$ .<sup>32,34</sup> This leads to a reduced transition probability of

$$B(E2, 2' \rightarrow 2)/B(E2, 2' \rightarrow 0) = 53;$$

i.e., the transition to the first  $2^+$  state is enhanced by

<sup>31</sup> W. V. Prestwich and R. E. Coté (private communication).  
<sup>32</sup> T. Tamazaki, H. J. Regemi, and M. Sakai, J. Phys. Soc. Japan **15**, 957 (1960).

<sup>33</sup> E. Eichler, R. L. Robinson, G. D. O'Kelley, and N. R. Johnson, Bull. Am. Phys. Soc. **6**, 228 (1961).

<sup>34</sup> D. P. Grechukhin, Nucl. Phys. **40**, 442 (1963).

TABLE VI. Determination of the neutron-separation energy  $E_N$  of (Ge<sup>73</sup>+*n*) from the relation  $E_N = E_\gamma + E_R + E_L$ , where  $E_\gamma$  is the  $\gamma$ -ray energy,  $E_R$  is the nuclear recoil energy, and  $E_L$  is the level energy.

$E_\gamma$ (keV)	$E_R$ (keV)	$E_L$ (keV)	$E_N$ (keV)
$9606.0 \pm 1.7$	0.7	$596.3 \pm 0.4$	$10\ 203.0 \pm 1.8$
$8997.7 \pm 1.4$	0.6	$1204.9 \pm 0.6$	$10\ 203.2 \pm 1.5$
$8736.4 \pm 1.3$	0.5	$1466.2 \pm 0.6$	$10\ 203.1 \pm 1.5$
			$E_N = 10\ 203.1 \pm 0.9$

a factor of 53 over the transition to the  $0^+$  ground state. The Ge<sup>74</sup> nucleus is, in this respect, more like the nearby even-even nuclei with larger mass numbers than it is like those with smaller mass numbers. Among the nearby lighter nuclei, this branching ratio is 2-10 times as large.

#### 4. 1460.2-keV Level

The  $4^+$  spin and parity of the 1466.2-keV level was established from measurements of the angular distribution of scattered protons and from Coulomb-excitation measurements. The level can consequently be reached from the capture state by  $M1$  radiation, which has a higher transition probability than quadrupole or higher multipole radiation. The observed direct transition is indeed moderately strong and probably contains a large fraction of  $M1$  radiation.

The level energy was obtained from the 1204.9-keV excitation energy and from the mean value of the separation between the 1204.9- and 1466.2-keV levels, as determined from the differences between the pairs of  $\gamma$  rays connecting these two levels to a common level. The level decays to the  $2^+$  state at 596.3 keV through the very strong 869.9-keV  $\gamma$  ray. The transition to the second  $2^+$  state was not seen.

#### 5. 1486-keV Level

This level was seen by Darcey,<sup>3</sup> who determined the  $0^+$  spin and parity from the angular distribution of scattered protons. No direct evidence for this level was found in the (*n*,  $\gamma$ ) data. An upper limit of 0.003% can be placed on a transition from the capture state. The strongest possibility of a connection to a lower level, namely, to the first  $2^+$  state, was obscured by the Compton edge of the strong 1103.4-keV  $\gamma$  ray and by the high-energy wing of the 869.9-keV transition. This wing did show some distortion, indicating a possible  $\gamma$  ray at 882.2 keV and an excitation energy of  $1478.5 \pm 1.3$  keV. The next most likely connection with states below 3 MeV involves the 1057.2-keV  $\gamma$  ray from the 2539.3-keV level and suggests a level energy of  $1482.1 \pm 1.3$  keV. Neither the 882.2- nor the 1057.2-keV  $\gamma$  ray can be fitted with certainty into the level scheme, and neither is included in Fig. 8.

TABLE VII. Branching ratio  $I_\gamma(609 \text{ keV})/I_\gamma(1205 \text{ keV})$  from the 1204.9-keV level in  $\text{Ge}^{74}$ , where  $I_\gamma$  is the  $\gamma$ -ray intensity.

This work $\text{Ge}^{73}(n, \gamma)\text{Ge}^{74}$	Eichler <i>et al.</i> <sup>a</sup>		Yamazaki <sup>b</sup>
	$\text{Ga}^{74} \rightarrow \text{Ge}^{74}$ $\beta$ decay	$\text{As}^{74} \rightarrow \text{Ge}^{74}$ $\beta$ decay	$\text{As}^{74} \rightarrow \text{Ge}^{74}$ $\beta$ decay
1.93±0.27	2.1±0.81	1.9±0.75	1.7±0.37

<sup>a</sup> References 2 and 33.<sup>b</sup> Reference 32.

### 6. 1697.7- and 1699.9-keV Levels

Two separate levels are suggested near 1700 keV. The transition from the capture state to the 1699.9-keV level was comparable in strength to the direct population of the  $4^+$  level at 1466.2 keV. Assuming this to be a dipole transition,  $M1$  or  $E1$ , restricts the possible spin of the level to the range  $J=3-6$ . However, the 1699.9-keV level decays to the  $2^+$  first excited state through the very strong 1103.4-keV  $\gamma$  ray. Since this deexcitation is most likely  $E1$ ,  $E2$ , or  $M1$  radiation, the spin and parity of the 1699-keV level is further limited to  $J^\pi=3^\pm$  or  $J=4^+$ . For these possible assignments, one might expect to see transitions from the 1699.9-keV level to the  $4^+$  state and to the second  $2^+$  state. A strong  $\gamma$  ray is present at  $493.0 \pm 0.8$  keV; and according to Weitkamp's  $(n, \gamma)$  data,<sup>11</sup> there may be a  $\gamma$ - $\gamma$  coincidence between the  $\gamma$  rays at 7.5 MeV, 1.0 MeV, and 0.6 MeV. This would be consistent with placing the 493.0-keV  $\gamma$  ray between the 1699.9- and 1204.9-keV levels except that the energy match is poor; the level separation, based on three independent  $\gamma$ -ray energy differences, is  $495.0 \pm 0.8$  keV. Consequently, the 493.0-keV line disagrees with the level spacing by  $2.0 \pm 1.1$  keV and possibly obscures the actual transition between these levels. The other possible transition, that to the  $4^+$  level at 1466.2 keV, would be at 233.7 keV—again in a region where the spectrum is not well defined.

The 493.0-keV  $\gamma$  ray appears with such strength that one would expect it to be somewhere between the low-lying states. Weitkamp's coincidence data suggest that it and the 1001.7-keV  $\gamma$  ray are in cascade between the 1204.9- and 2699.1-keV levels. The weaker intensity of the 1001.7-keV line indicates that this  $\gamma$  ray feeds the intermediate level while the stronger 493.0-keV line depletes it. The level energy from this combination is  $1697.7 \pm 1.0$  keV. This second tentative level postulated near 1700 keV, independent of the 1699.9-keV level, would also explain Weitkamp's observation of no coincidence between the 1001.7-keV line and either the 1103.4- or the 869.9-keV  $\gamma$  ray. This lack of coincidence would eliminate both the 1699.9- and 1466.2-keV levels as possible connections.

### 7. 2168.3-keV Level

The level at 2168.3 keV is populated from the capture state by a strong transition at 8034.5 keV. The

$\gamma$ -ray intensity, 0.624%, is similar to the intensity of the transitions to the 1699.9- and 1466.2-keV levels. Since it also decays to the second  $2^+$  state at 1204.9 keV, an argument identical to the one applied to the 1699.9-keV level limits its probable spin and parity to  $J=3^\pm$  or  $4^+$ . The transitions to the  $4^+$  level at 1466.2-keV and to the level at 1699.9 keV, with  $J^\pi=3^\pm$  or  $4^+$  probable, are consistent with this assignment, as is the nonobservance of a transition to the  $0^+$  level at 1486 keV, since the latter would require an  $E3$  or  $M3$  transition.

The 1577.2-keV line, the most likely candidate for a transition to the first  $2^+$  state, is energetically  $4.8 \pm 1.4$  keV too large and is not included here. A line of energy  $1590 \pm 10$  keV is included in the scheme of Eichler *et al.*<sup>2</sup> It is possible that the 1577.2-keV  $\gamma$  ray from the  $(n, \gamma)$  reaction (not shown in Fig. 8) is not identical to the 1590-keV  $\gamma$  ray seen in the  $\text{Ga}^{74} \rightarrow \text{Ge}^{74}$   $\beta$  decay. This conclusion is supported by considering the relative strengths (Table VIII) of the  $\gamma$  rays that may depopulate the level. The disparity of the results for the 1577.2-keV line is significant; it is barely more than a seventh of the  $\gamma$ -ray intensity expected from the  $\beta$ -decay results. The 1590-keV  $\gamma$  ray in the  $\beta$ -decay experiment therefore cannot proceed from the 2168.3-keV level and must come from a level that is not appreciably populated in the  $(n, \gamma)$  reaction.

### 8. 2200.2-keV Level

This state decays through the 732.6-keV  $\gamma$  ray to the  $4^+$  level at 1466.2 keV, and to the  $0^+$  ground state and the  $2^+$  first excited state by weak low-energy  $\gamma$  rays of energy  $2200.0 \pm 1.3$  and  $1604.3 \pm 2.2$  keV, respectively. This determines a spin and parity of  $J^\pi=2^+$  for the 2200.2-keV level since octupole transitions would be required for anything else. A weak direct transition (8002.2 keV) from the neutron-capture state to this state was observed in this experiment. Its  $\gamma$ -ray strength,  $I_\gamma=0.007\%$ , is consistent with the assumption of  $E2$  multipolarity.

A level at  $2200 \pm 20$  keV is populated in the  $\beta$  decay of  $\text{As}^{74}$ . The strengths of the transitions to the ground state and to the first and second excited states are in

TABLE VIII. Relative strengths of the possible transitions from the 2168.3-keV level in  $\text{Ge}^{74}$ .

$E_\gamma$ (keV)	$I_\gamma(E_\gamma)/I_\gamma(963.5)$	
	This work $\text{Ge}^{73}(n, \gamma)\text{Ge}^{74}$	Eichler <i>et al.</i> <sup>a</sup> $\text{Ge}^{74} \rightarrow \text{Ge}^{74}$ $\beta$ decay
468.4	0.12	(?)
702.7	0.52	0.69
963.5	1.00	1.00
1577.2 <sup>b</sup>	0.10	0.67

<sup>a</sup> Reference 2.<sup>b</sup> Not included in the level scheme (Fig. 8).



the ratio of 2:1:17, according to Girgis and van Lieshout.<sup>35</sup> These intensity ratios are consistent with those observed in this experiment, but the energy of the strongest member (the possible transition to the second 2<sup>+</sup> state) is not. The energetically closest  $\gamma$  ray with the appropriate intensity is the (1001.7 $\pm$ 0.8)-keV line. This is 6.4 $\pm$ 1.4 keV too large for the level spacing and therefore is not included as part of the decay of the 2200.2-keV level. As mentioned earlier, the 1001.7-keV line probably feeds the tentative level at 1697.7 keV. The alternative is a level at 2206.6 keV, fed by the 493.0-keV  $\gamma$  ray from the 2699.1-keV level, and depleted by the 1001.7-keV transition to the 1204.9-keV level. This possibility is rejected by the intensity imbalance between the strong 493.0-keV line and the weaker 1001.7-keV line.

#### 9. 2539.3-keV Level

In his studies of the Ge<sup>74</sup>(*p*, *p'*)Ge<sup>74</sup> reaction, Darcey<sup>3</sup> inferred a spin and parity assignment of  $J^\pi=3^-$  for a level at 2537 $\pm$ 10 keV on the basis of the angular distribution of scattered protons, and Dickens *et al.*<sup>4</sup> earlier suggested a 3<sup>-</sup> level at 2.61 MeV. The level energy found in the present experiment is 2539.3 $\pm$ 0.6 keV. It is weakly populated from the capture state; the strength of the transition is similar to that of the one going to the 2<sup>+</sup> level at 596.3 keV. This level is close to a level populated in the  $\beta$  decay of Ga<sup>74</sup>. The relative intensities of the  $\gamma$  rays from the two reactions are shown in Table IX. The intensities suggest that the  $\gamma$  ray at 2.55 $\pm$ 0.02 MeV observed in the  $\beta$  decay of Ga<sup>74</sup> is not the ground-state transition of the 2539.3-keV level, since it is not measurable in the (*n*,  $\gamma$ ) work—neither here nor in the work of Weitkamp *et al.*<sup>11</sup> The  $J^\pi=3^-$  assignment would necessitate octupole transitions to the ground state and to the 1486-keV level; consequently, they are expected to be undetectable. The lack of transitions to the states at 1699.9 keV and 2168.3 keV, whose level spin is likely to be  $J^\pi=3$  or 4<sup>+</sup>, may indicate a difference between the character or configuration of these levels and the 2539.3-keV state.

#### 10. 2574.1-keV Level

The level at 2574.1 keV, first observed by Darcey<sup>3</sup> at 2575 $\pm$ 7 keV, is confirmed in this work by a direct transition from the neutron-capture state. This transition has not been reported previously. The level decays by the 1108.9-keV  $\gamma$  ray which, with the 1103.4-keV line, composes an intense doublet at 1.1 MeV. The doublet nature of this peak is clear from its width at half-maximum height, which was 20% larger than the width of the nearby 1204.9-keV full-energy peak.

#### 11. 2672.4-, 2695.8-, and 2699.1-keV Levels

The level at 2672.4 keV has not been reported before. It is weakly populated from the neutron-capture

<sup>35</sup> R. K. Girgis and R. van Lieshout, *Physica* **25**, 668 (1959).

TABLE IX. Relative strengths of the possible transitions from the 2539.3-keV level.

$E_\gamma$ (MeV)	$I_\gamma(E_\gamma)/I_\gamma(1.335)$	
	This work Ge <sup>73</sup> ( <i>n</i> , $\gamma$ )Ge <sup>74</sup>	Eichler <i>et al.</i> <sup>a</sup> Ga <sup>74</sup> $\rightarrow$ Ge <sup>74</sup> $\beta$ decay
1.335	1.0	1.0
1.943	4.0	1.3
2.551 <sup>b</sup>	<0.1	0.7

<sup>a</sup> Reference 2.

<sup>b</sup> This line is seen in the  $\beta$  decay of Ga<sup>74</sup> but not in the Ge<sup>73</sup>(*n*,  $\gamma$ )Ge<sup>74</sup> reaction and is not included in the decay scheme (Fig. 8).

state and has only one observable connection to the lower levels, i.e., the 2075.3-keV transition to the first 2<sup>+</sup> state.

Another level at 2695.8 keV was suggested by the close energy fit of three possible connections to the first and second 2<sup>+</sup> states, and to the 4<sup>+</sup> level at 1466.2 keV. Only two other sets of  $\gamma$  rays and energy levels fit together as well to suggest a new level in the 2–3-MeV range, and those two provided an unsatisfactory intensity balance. The effort to place an upper limit on the transition to the 2695.8-keV level from the capture state was hindered by the proximity of the moderately strong, direct transition to the next level at 2699.1 keV. Each of the three connections of the 2695.8-keV level differ from the level spacing to the 2699.1-keV level by at least 3.0 $\pm$ 1.4 keV and were consequently ruled out as originating from that level. It is not clear which of the two levels at 2695.8 and 2699.1 keV is excited in the (*p*, *p'*) reaction reported by Darcey, since his determination of the level energy is 2695 $\pm$ 10 keV.

The level at 2699 $\pm$ 1 keV decays by a 530.9-keV  $\gamma$  ray to the state at 2168.3 keV. A transition to the ground state, though energetically possible, is doubtful because it would limit the spin of the 2699.1-keV state to values  $J \leq 2$ , while the strong transition from the capture state to this level suggests  $J \geq 3$ . This problem also exists with the energetically possible ground-state transition from the 2833.2- and 2978.1-keV levels. The large uncertainty in these  $\gamma$ -ray energies leads to a large probability of an accidental energy fit. They are consequently not included in the level scheme.

#### 12. 2833.2-, 2929.2-, 2939.7-, and 2978.1-keV Levels

The state at 2833.2 keV is populated from the neutron-capture state, is seen in the (*p*, *p'*) reaction, strongly decays to the 1699.9-keV level, and has a weak transition connecting it to the first excited state. The connection suggested by Weitkamp to the 1204.9-keV level would come nearest to having the energy of the 1635.8-keV  $\gamma$  ray; but the latter, as determined here, is energetically 7.5 $\pm$ 1.9 keV too large.

Another state at 2929.2 keV was suggested by the

observation of a weak high-energy  $\gamma$  ray from the capture state. It has energetically possible connections to lower levels at 1699.9 keV and 596.3 keV.

The strongest high-energy  $\gamma$  ray populates the level at  $2939.7 \pm 0.5$  keV. Although this may be the state that both Eichler and Ythier saw at 2.95 MeV, a very strong transition to the first excited state is suggested in all of the  $\beta$ -decay work but is missing in the  $(n, \gamma)$  reaction; this is also true of the weaker transitions to the ground state and to the 1204.9-keV level. The connections by way of the 1473.5- and 771.2-keV  $\gamma$  rays, observed by Girgis and van Lieshout, energetically match the level spacings, as does a connection to the proposed level at 2200.2 keV. But the 2.35-MeV  $\gamma$  ray should be 6–7 times as intense as the strong 1473.5-keV line, and would rank as the third most intense low-energy  $\gamma$  ray in the  $\text{Ge}^{74}$  spectrum. Its absence in the  $\text{Ge}^{73}(n, \gamma)\text{Ge}^{74}$  reaction requires a reinterpretation of the  $\beta$ -decay results and the placing of the 2.35-MeV  $\gamma$  ray elsewhere in the scheme.

The last level below 3 MeV was found to be at  $2978.1 \pm 0.5$  keV. It is strongly populated from the capture state, and two connections to lower levels fit well energetically. The 1511.8- and 809.8-keV  $\gamma$  rays were also observed by Weitkamp. A possible transition to the second excited state was interpreted as the double-escape peak of the 2788-keV  $\gamma$  ray, and not as the full-energy peak necessary for the connection.

## VI. CONCLUSIONS

Several significant additions to the energy-level scheme of  $\text{Ge}^{74}$  result from this experiment. Three new levels at 2574.1, 2672.4, and 2929.2 keV have been established by direct transitions from the cap-

ture state and by deexcitations to lower states. A fourth new state at 2695.8 keV was suggested by the close energy correlation between three measured  $\gamma$ -ray energies and lower levels. The spins and parities of three of the states, at 1699.9, 2168.3, and 2200.2 keV, have been limited by the measured intensities of associated  $\gamma$  rays. Two transitions from the capture state to the previously known levels at 2200.2 and 2539.3 keV were first reported. The uncertainties in the energies of the  $\gamma$  rays and of the levels have been reduced to less than 1 keV in most cases. This has revealed, in one case, a 2-keV discrepancy between a level spacing (the  $1699.9 \rightarrow 1204.9$  keV spacing) and the energy of a  $\gamma$  ray (at 493.0 keV) which had been suggested as the connection. A fifth new level is tentatively proposed to account for the 493.0- and 1001.7-keV transitions.

The energy structure and the sequence of spins and parities of the first five states of  $\text{Ge}^{74}$  seem to indicate a vibrational-type nucleus. The intensities of the  $\gamma$  rays measured here do not conflict with this interpretation. However, comparisons of the level scheme with the vibrational model, or with the asymmetric and symmetric rotor models, must be judged inconclusive until more information on the spins and parities of the upper states and the multipolarities of the transitions becomes available.

## ACKNOWLEDGMENTS

The authors wish to acknowledge the assistance of many members of the Argonne Physics Division, both in the experiment and in the completion of this paper. Particular thanks are due to Dr. Esther Segel for her council on the thesis and to George Thomas and James Specht for their technical aid.